# BENDING STRENGTH OF BEAMS WITH NON-LINEAR ANALYSIS

Pekka Salmi[1] and Asko Talja[2]

Rakenteiden Mekaniikka, Vol. 25
No 4 1992, ss. 50 - 67

## SUMMARY

Bending strengths of open cross-section beams cold-formed from high-strength steel (HSS) are determined with non-linear analysis. Two kinds of beams are studied. The short beams are for examining the bending resistance of cross-sections and the long beams for studing the lateral buckling of open sections. The beams are modelled with shell elements and non-linear FEM analyses are carried out to predict the strengths of the models. Both material and geometrical non-linearities are included in the analyses. The results are compared with experimental results.

## 1 INTRODUCTION

Steel members of moderately high slenderness have become widely used in modern engineering structures. The load capacity of such members is not easy to determine because of its dependence on a large number of parameters related to geometric and material properties. Initial imperfection, residual stresses and other irregularities have an effect on the behaviour of the member. A member may buckle locally before the ultimate load is reached, leading to a reduction in the load capacity. A base material of higher strength even increases these local instabilities owing to the higher slenderness. The design formulas available in design codes are mostly empirical. They have been

[1] Research Scientist, Technical Research Centre of Finland (VTT), P.O.Box 26, SF-02151 ESPOO, Finland

[2] Senior Research Scientist, Technical Research Centre of Finland (VTT), P.O.Box 26, SF-02151 ESPOO, Finland

developed or at least verified by experiments. When the amount of phenomena increases, the number of tests needed to verify calculations becomes often large. Experiments are very time-consuming and expensive to conduct. Hence some interest has arisen for predicting the strength of structures by simulating actual tests and expanding their results numerically.

Elastic buckling and non-linear analyses by finite element [2, 3, 7, 8] or finite strip methods [4, 5, 6, 9, 15] have been carried out. The applications used in the analyses are usually privately developed and not publicly available. Stability and static strength of structures can be studied with general finite element programs, when both material and geometrical non-linearities are modelled. The program should contain a method for analyzing post-critical response of the structure when the load factor decreases. Several generally available programs such as ABAQUS, ADINA and Nisa contain these capabilities. For this study the ABAQUS program [1] was chosen.

In this study the potential of the general-purpose finite element code is examined as a supplementary tool for the static bending test. Physical tests are simulated with non-linear analysis. In other words, a non-linear response is calculated for the models of the beams. The response of the model of the structure is analyzed and the maximum load-carrying capacity is determined from the equilibrium path. The beams are modelled using shell-elements. All effects like distortion of the cross-section during buckling and effects of local instabilities are noted with these kind of models. Boundary conditions and loadings are set to match those employed in the physical tests.

With the modelled tests the bending strength of singly symmetrical cold-formed beams is studied when they are loaded along the axis of symmetry [13]. The beams used in the tests are cold-formed from high-strength steel (HSS). The calculations of bending strength of cold-formed beams is divided into two groups on the basis of beam length. For short beams the cross-sectional bending strength, and for long beams lateral buckling strength is calculated. Tests were made to verify both cross-sectional (eight specimens) and lateral buckling strength (four specimens). In the analyses both cases also have details of their own in modelling.

## 2 EXPERIMENTAL INVESTIGATION

The bending strength is tested with four-point loading (figure 1). The tests were carried out in a 6000 kN MAN testing machine. The loading is transmitted to the test specimen through the compression platten of the testing machine and a stiff large-size hollow-section beam. The end supports are on the compression platten, which is lifted with the hydraulic cylinder against the loading points, which are supported by the stiff beam.

Especially in the lateral buckling tests some additional degrees of freedom were arranged in the support and loading points so that the buckling lengths could be determined. The main principle was that the bearings under the forces and the supports were free to move in the horizontal plane, but the rotation about the longitudinal axis was restrained. The other end support was restrained in the longitudinal direction. In the case of short beams, sideways translations and vertical rotations are both restrained under the forces and at end supports. In reality each individual degree of freedom was treated separately (figure 2).

To avoid the opening of the channel, the flanges were connected together with a bar. The bars were either under the forces or at supports depending on the position of the section. To avoid local crushing caused by reaction forces there were additional bearings both under the forces and at the supports. The bearing length was 100 mm.

A total of four different cross-sections were chosen; two c- and two hat-cross sections. The geometry of the sections is given by centre-line dimensions measured from the test specimens (figure 3 and table 1). Material thicknesses and the yield stresses are based on the longitudinal tension test results of flat-plate sections (table 3). In the table both lower and upper yield strengths are given. In those two cases where only one value is given, no exact limit value is found in the tension test. The value for 0.2-% permanent strain is given.

Three different test specimens of each cross-section were tested. The cross-sectional bending strength was determined in both directions, but the lateral buckling strength only in the direction that lips were pressed. The specimen lengths and other dimensions of the test arrangement (figure 1) are shown in table 2. The measured strengths and notes about deformations during the tests are also given in the table. Mode "P" means deflection failure in the plane, "T" means that torsion of the beam is also observed, "S" means stiffener buckling and "L" local deformations under the bearing. The force in the table is given for one loading point (figure 1).

More detailed information on the tests and test specimens modelled here are documented in the reference [13].

# 3 ANALYSIS MODEL

The strength of beams is determined on the basis of non-linear analysis. Both geometrical and material non-linearities are included. Geometrical non-linearity means that displacements caused by the loading lead to certain load-displacement responses of the model. The strength of the model can be determined from this response as the ultimate load in the loading history. A non-linear material model is included to model the loss of stiffness due to possible plastic strains.

When the strength of the structure is studied with non-linear analysis, an initial disturbance is needed in some structures. For instance, with the Euler column a small parallel force or initial imperfection is needed when the non-linear response is analysed. In more complex structures the effect of a small force is difficult to control and the imperfection shape has many possible forms. It is difficult to decide what is the most critical one. This can be done with buckling analysis. General finite element codes contain the possibility of performing buckling analysis to determine buckling loads and modes. Although there are strict rules on when results of the buckling analysis are applicable in analyzing the strength of structures, the buckling modes represent the displacement fields possible for the structure [17]. The shape of the lowest eigenvalue describes the most potential displacement field of the structure.

With cold-formed beams the first shape is not always the critical one, because there can be a local buckling shape. The number of shapes can be reduced to certain possible shapes [14]. An advantage of using the shape from buckling analysis is that this mode can very easily be included in the model. In this way the load-displacement response of the model is controlled and the strength corresponds to that of the specific stability mode. This analysis procedure is tested for axially and eccentric compressed HSS channels [13, 14]. The results obtained are reasonable.

## 3.1 MODELS AND CONSTRAINTS

The beams are modelled with shell-elements. Therefore all cross-sectional distortions and local buckling effects are possible in the model during the loading. Nodes are placed on the centre-line of the cross-section. Dimensions used in the models are given in table 1. Cross-sections are modelled right-angled.

Owing to the use of shell-elements the models become rather large, which increases the solution time. The economical use of elements is worth studying especially in the non-linear analysis, when several iterations and loading steps has to be solved. The element mesh used also has an important effect on the accuracy of results. In these kinds of analysis no stress concentrations need to be modelled, but it is important that the stiffness of structures is modelled as accurately as possible.

These cold-formed beams are of a prismatic nature. The cross-sectional division of elements also has an effect in the longitudinal element division, because element dimensions have to be moderate. When parabolic shell-elements are used, the displacement field in local plate buckling can be modelled accurately with four elements. In the unstiffened lips, one or two elements are used. In the longitudinal direction the length/width ratio of elements is kept under three. This kind of element division is also sufficient, when material non-linearity is included in the model [11].

Loadings and constraints have to be arranged equal to those in the actual test arrangement. In the test set-up stiffening steel bearings are used to avoid local crushing of the beam. In the models these stiff plates are assumed to move linearly. This is arranged with constraint equations. The equations are modelled in the edges of the cross-section so webs and flanges are not stiffened unnecessarily. The loading and constraints are placed in the middle node of these bearing regions. The bars, which are welded in the beams to avoid the opening of the cross-section, are modelled with trusses. As an example, in figures 4 and 5 the whole models of test cases H1/MR1 and C2/MR2 are shown.

## 3.2 MATERIAL MODEL

In a general finite element code, such as the ABAQUS program in this case, the normal elastic-plastic material model is assumed to be bilinear and the Bauschinger effect is not included. Von Mises yield function is usually used in these material models [1].

In these analyses, standard longitudinal tension test results were available for each modelled test specimen. The ideally elastic-plastic material model (figure 6) describes the measured stress-strain relationships rather well . As the limit value the upper yield stress is used. Material constants used are the modulus of elasticity 210 GPa and Poisson's ratio 0.3.

## 3.3 INITIAL IMPERFECTIONS

Initial imperfection is used to lead the load-displacement response of the model to a certain shape of stability loss. With compressed structures some kind of disturbance is essential, because loading itself has no distorting effect on the model. Bending of the structure may present such an effect itself. Because of the shear forces induced by the loading, the short beams need no additional imperfections [11]. When lateral buckling of long beams is modelled, the symmetrical deformation caused by the loading does not give rise to the non-symmetrical buckling phenomenon. Imperfection is needed to disturb the model. The shape of imperfection is predicted by buckling analysis. Figure 7 shows the first mode shapes of two test cases, C2/MR3 and H1/MR3. The buckling loads from analyses are 119 kN and 83 kN, given as the force for one loading point (figure 1).

The size of imperfection can be decided for instance on the basis of actual measured imperfection or by the tolerances given in design codes. In this way some guidance can be obtained, but the absolute value is not reached. For instance, in the case when lateral buckling is modelled, should the size of imperfection be decided on cross-sectional tolerances or longitudinal ones? Some kind of estimate can be calculated with the formula for manufacturing tolerance in [16]. The size of "global" imperfection obtained from it is about two wall thicknesses in these cases. The Finnish standard for cold-rolled steel sections [12] gives as a maximum allowable rotation of the section 1 degree/m. Actually the initial imperfections should also include some kind of equivalent value of the internal imprefections, which cannot otherwise be modelled (e.g. residual stresses).

As an example the specimen C2/MR3 is analyzed with different imperfection sizes in figure 8. The shape of imperfection used is the first buckling mode (figure 7). The imperfection size is notified with respect to the wall thickness of the section and as the rotation angle of the middle cross-section, which describes the imperfection size better. In these analyses, the ideally elastic-plastic material model is used. Without any imperfection the strength of the model is 122 kN. Figure 9 shows deformed shapes of models at the end of analysis with no imperfection and with lateral buckling imperfection. Displacements in the figure are of the actual size.

# 4 RESULTS AND COMPARISON

Models were analyzed with the ABAQUS program using the modified Riks method [10], which is also capable of analyzing the post-buckling range. In the analyses, that model cross-sectional bending tests, loading is restricted to 15 steps. In lateral buckling analyses 20 steps are used. These analyses were carried out in the Cray X-MP supercomputer. Analyses of cross-sectional bending strength took from 10 to 20 minutes CPU-time when symmetry conditions were utilized. In lateral buckling analyses models were significantly larger. These analyses took from one to one and a half hours of CPU-time.

When cross-sectional bending strength was determined no additional imperfection is in this case needed. In figures 10, 11, and 12 three different cases, C2/MR1, C1/MR1 and H1/MR2, are compared. The loading itself causes the disturbance, as can be seen from the lateral displacements and cross-sectional distortions shown in figures 10, 11 and 12. The material model used was the ideally elastic-plastic material model described earlier. The symmetry conditions were used in the analyses and only a half of the beam was modelled. The comparisons of strengths are given in table 4.

In the analysis of lateral buckling strength, the buckling analysis was performed to determine the shape of initial imperfection. In all four cases the first buckling mode shows lateral buckling [11]. These modes are used as the shape of imperfection in the non-linear analysis. The material model was the ideally elastic-plastic model explained before. Figures 13 and 14 show the displacements of beams C2 and H1. In the lateral buckling tests, the lateral displacement and rotation of the cross-section are compared. Compared strengths like the displacements in figures 13 and 14 are calculated with an imperfection size of two wall thicknesses. The case C1 was the exception not showing rotation of cross-section in the test. This case was analysed without any imperfection and the strength of the model was of the same magnitude with an imperfection of one wall thickness. Results are given in table 5.

# 5 CONCLUSIONS

Cross-sectional bending strength can be determined with a rather simple model; the ideal elastic-plastic material model with no imperfection gives a precision of 12 percent in the accuracy of strength predictions. With those specimens where the difference was over 10 percent, local crushing was observed in the tests. The rather large corner radius was not modelled.

Non-symmetrical imperfection is needed in the lateral buckling analyses. The shape of imperfection may be determined by buckling analysis. When the size of imperfection is two wall thicknesses the lateral buckling strength of the model of the beam compared to the tested beam is overestimated by as much as 12 percent. The decision concerning imperfection size in the non-linear analysis needs further discussion.

Computational costs with these kinds of models are rather large, but the development in computer calculation capacity has been so vast, that soon even lateral buckling analyses can be performed in personal computers.

# ACKNOWLEDGEMENTS

This study was made as the thesis for a Master's degree at the Helsinki University of Technology. The work was supported by the Finnish Association of Steel Structures (TRY). Modelled tests were made as a part of a research programme on the use of high-strength steels (HSS) in building constructions. The main purpose of the programme is to develop design rules for HSS steel structures. The programme is carried out at the Laboratory of Structural Engineering of the Technical Research Centre of Finland (VTT). Test sections were supplied by Rautaruukki Oy's Toijala Works.

# APPENDIX I - REFERENCES


1. ABAQUS, Version 4.8. User's Manual. Providence, RI 1989, Hibbitt, Karlsson & Sorensen, Inc.

2. Basu, P. K. & Akhtar, M. N. Interactive and local buckling of thin-walled members. Thin-Walled Structures 12(1991), pp. 335 - 352.

3. Chan, S. L., Kitipornchai, S. & Al-Bermani, F. G. A. Elasto-plastic analysis of box-beam columns including local buckling effects, Journal of Structural Engineering 117(1991)7, pp. 1946 - 1962.

4. van Erp, G.M. Advanced buckling analysis of beams with arbitrary cross sections. PhD Thesis, Technische Universiteit Eindhoven. Enschede 1989. 102 p.

5. Guo, Y. L. & Chen, S. F. Elasto-plastic interaction buckling of cold-formed channel columns. Journal of Structural Engineering 117(1991)8, pp. 2278 - 2298.

6. Hancock, G. J., Davids, A. J., Key, D. W., Lau, S. C. W. & Rasmussen, K. J. R. Recent developments in the buckling and non-linear analysis of thin-walled structural members. Thin-Walled Structures 9(1990)2, pp. 309 -338.

7. Jönsson, J. Recursive finite elements for buckling of thin-walled beams. Lyngby 1990, Technical University of Denmark, ABK - Department of Structural Engineering, Serie R, no. 263. 204 p.

8. Kitipornchai, S., Al-Bermani, F. G. A. & Chan, S. L. Geometric and material nonlinear analysis of structures comprising rectangular hollow sections. Eng. Struct. 10(1988)1, pp. 13 - 23.

9. Rasmussen, K. J. R. & Hancock, G. J. Nonlinear analysis of thin-walled channel section columns. Thin-Walled Structures 13(1992)1-2, pp. 145 - 176.

10. Riks, E. An incremental approach to the solution of snapping and buckling problems. Int. J. Solids Struct. 15(1978)7, pp. 529 - 551.

11. Salmi, P. Avoimien muotoprofiilipalkkien taivutuskantokyvyn määrittäminen elementtimenetelmällä (Determination of bending strength of open cross-section beams with finite element method) (in Finnish). Master's thesis, Helsinki University of Technology, Espoo 1992. 77 p.

12. SFS 5484. Cold rolled steel sections. Dimensions and sectional properties. Finnish Standards Association, Helsinki 1989. 7 p.

13. Talja, A. Design of cold-formed HSS-channels for bending and eccentric compression. Bending in the plane of symmetry. Espoo 1992, Technical Research Centre of Finland, will be published in the Technical Notes.

14. Talja, A., Salmi, P. & Vähä-Pietilä, K. Elementtimenetelmän käyttö poimulevyjen ja muotosauvojen pistekuorma- ja puristuskestävyyden määrittämisessä (The use of finite element method in the determination of the strength of cold-formed sheetings and columns for consentrated load or compression) (in Finnish). Espoo 1991, Technical Research Centre of Finland, Technical Notes 1257. 57 p. + liitteet 39 p.

15. Yanlin, G. & Shaofan, C. Postbuckling interaction analysis of cold-formed thin-walled channel sections by finite strip method. Thin-Walled Structures 11(1991)3, p. 277 - 289.

16. Yu, W. W. Cold-formed steel design. New York 1985, John Wiley & Sons. 545 p.

17. Zienkiewicz, O. C. The Finite Element Method. 3. p. London 1977, McGraw-Hill Book Company (UK) Limited. 787 p.

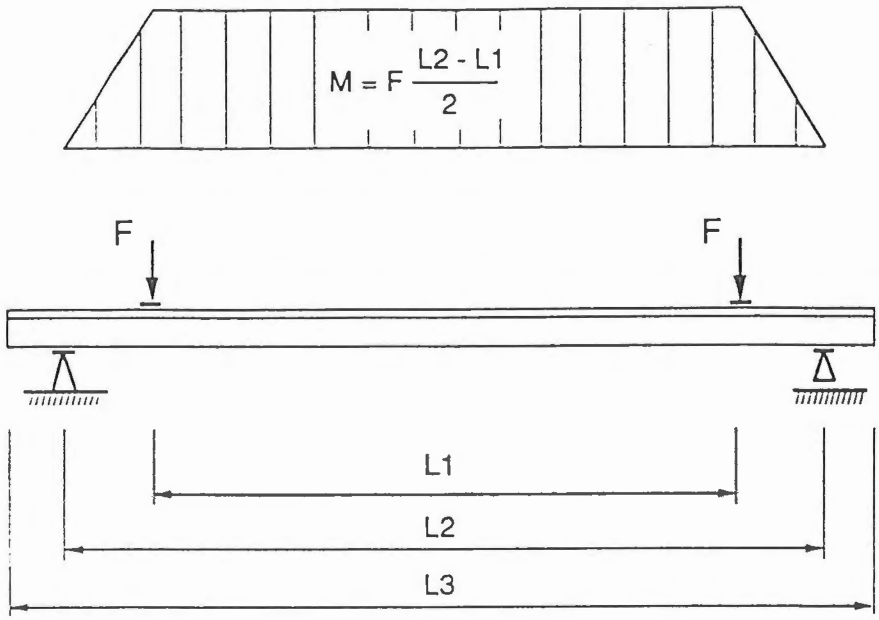


*Figure 1.*

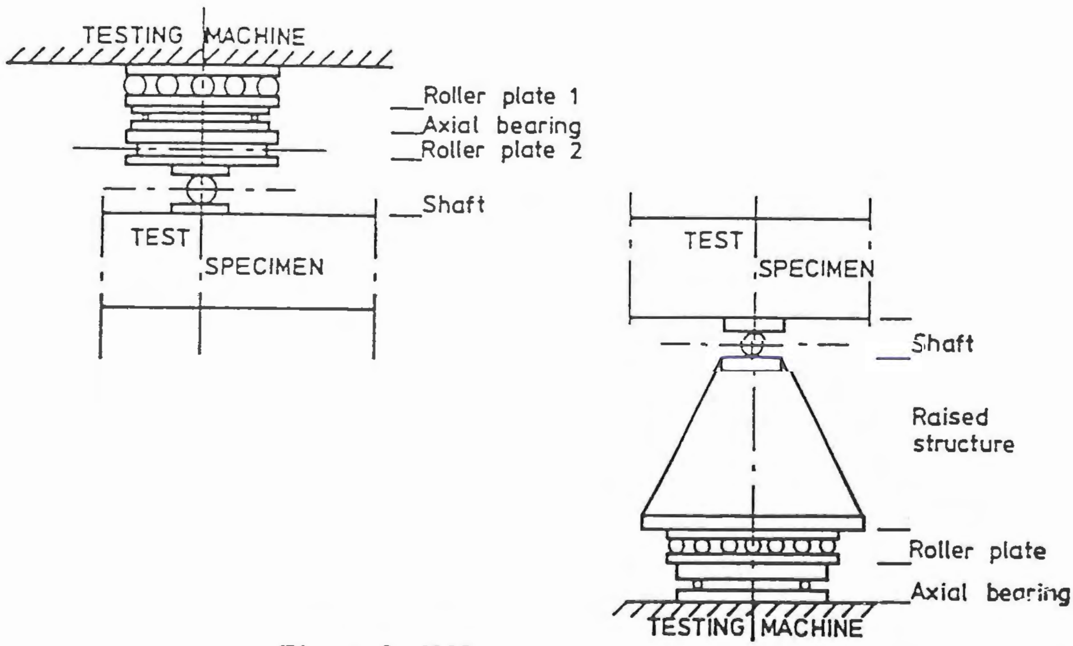


*Figure 2. [13]*

*Table 1.*

| Cross-section | t [mm] | a [mm] | b [mm] | c [mm] | r [mm] |
|---|---|---|---|---|---|
| C1 | 3,96 | 200,2 | 79,4 | 25,6 | 3,9 |
| C2 | 4,93 | 129,9 | 129,3 | 23,3 | 1,9 |
| H1 | 5,95 | 152,0 | 150,4 | 36,0 | 8,6 |
| H2 | 5,95 | 132,1 | 130,1 | 58,3 | 8,4 |

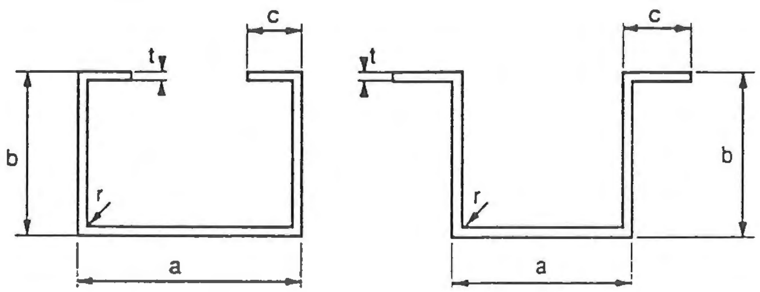


*Figure 3.*

*Table 2.*

| Specimen | L1 [mm] | L2 [mm] | L3 [mm] | F [kN] | Failure mode |
|---|---|---|---|---|---|
| C1/MR1 | 500 | 1000 | 1500 | 71,5 | P + S |
| C1/MR2 | 500 | 1000 | 1500 | 76,0 | P |
| C1/MR3 | 4000 | 4500 | 5000 | 57,0 | P + S |
| C2/MR1 | 500 | 1000 | 1500 | 158,0 | P + S |
| C2/MR2 | 500 | 1000 | 1500 | 195,0 | P + L |
| C2/MR3 | 4000 | 4500 | 5000 | 84,5 | T + S |
| H1/MR1 | 1000 | 2000 | 2500 | 141,5 | P + S |
| H1/MR2 | 1000 | 2000 | 2500 | 185,0 | P + L |
| H1/MR3 | 4000 | 5000 | 6000 | 71,0 | T |
| H2/MR1 | 1000 | 2000 | 2500 | 142,0 | P + S |
| H2/MR2 | 1000 | 2000 | 2500 | 163,5 | P + L |
| H2/MR3 | 4000 | 5000 | 6000 | 59,0 | T |

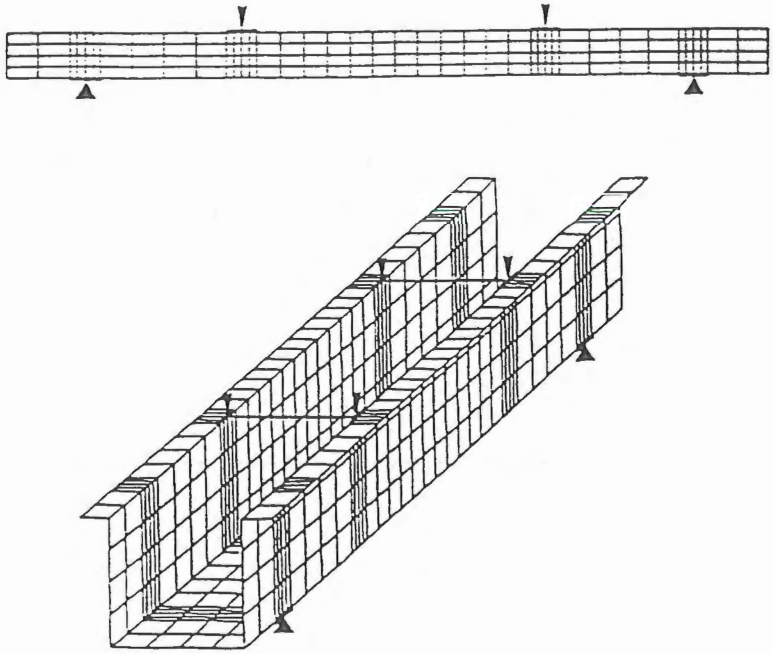

*Figure 4. H1/MR1*

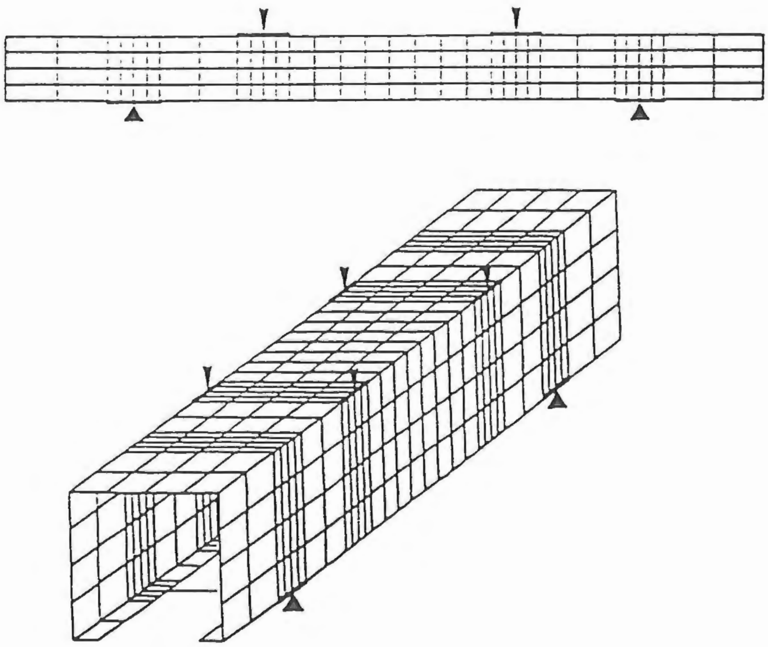

***Figure 5. C2/MR2***

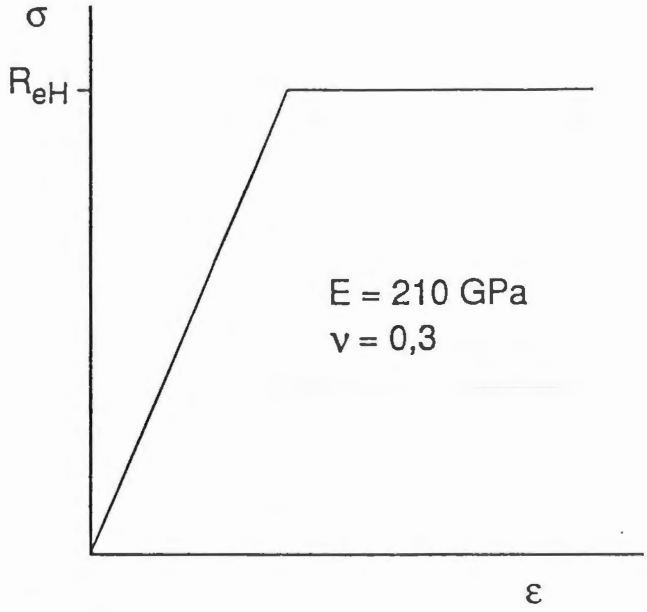


*Figure 6.*

*Table 3.*

| Specimen | $R_{eL}$ [MPa] | $R_{eH}$ [MPa] | Specimen | $R_{eL}$ [MPa] | $R_{eH}$ [MPa] |
|---|---|---|---|---|---|
| C1/MR1 | 555 | 557 | H1/MR1 | 664 | 671 |
| C1/MR2 | 546 | 556 | H1/MR2 | — | 660 |
| C1/MR3 | 546 | 559 | H1/MR3 | — | 660 |
| C2/MR1 | 556 | 571 | H2/MR1 | 652 | 666 |
| C2/MR2 | 556 | 571 | H2/MR2 | 623 | 632 |
| C2/MR3 | 549 | 559 | H2/MR3 | 623 | 632 |

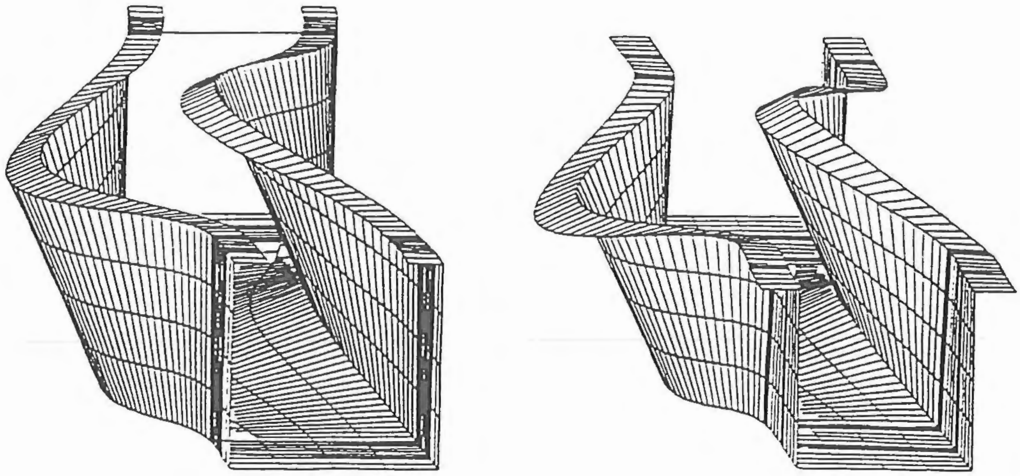

*Figure 7. (a) C2/MR3 and (b) H1/MR3*

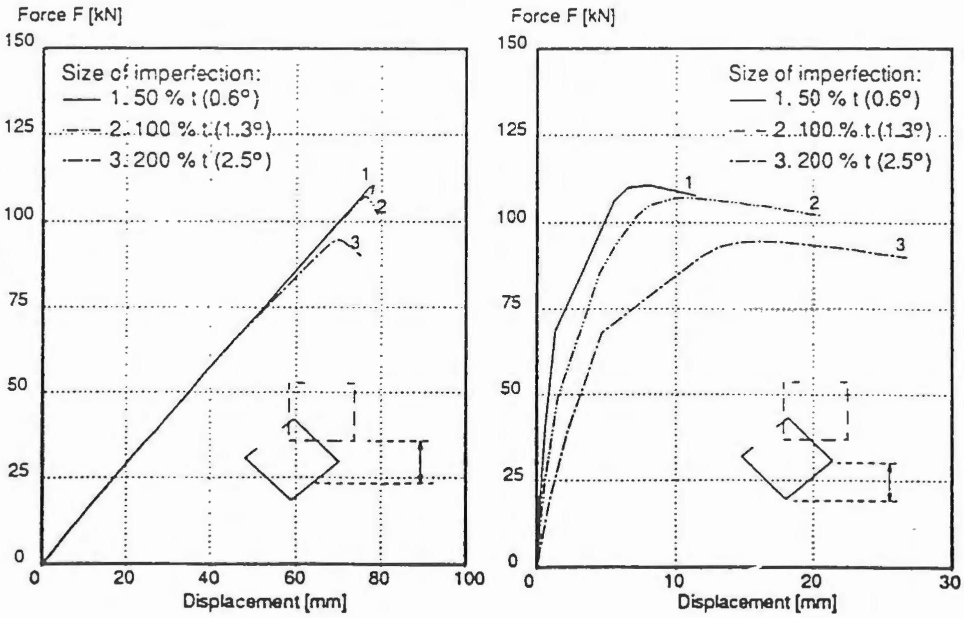


***Figure 8. C2/MR3***

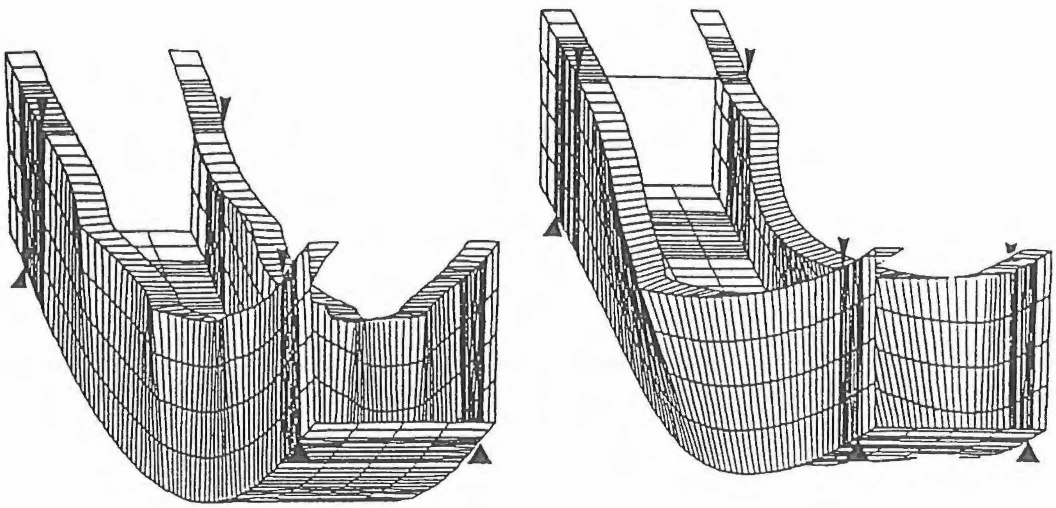

*Figure 9. (a) No imperfection and (b) with imperfection*

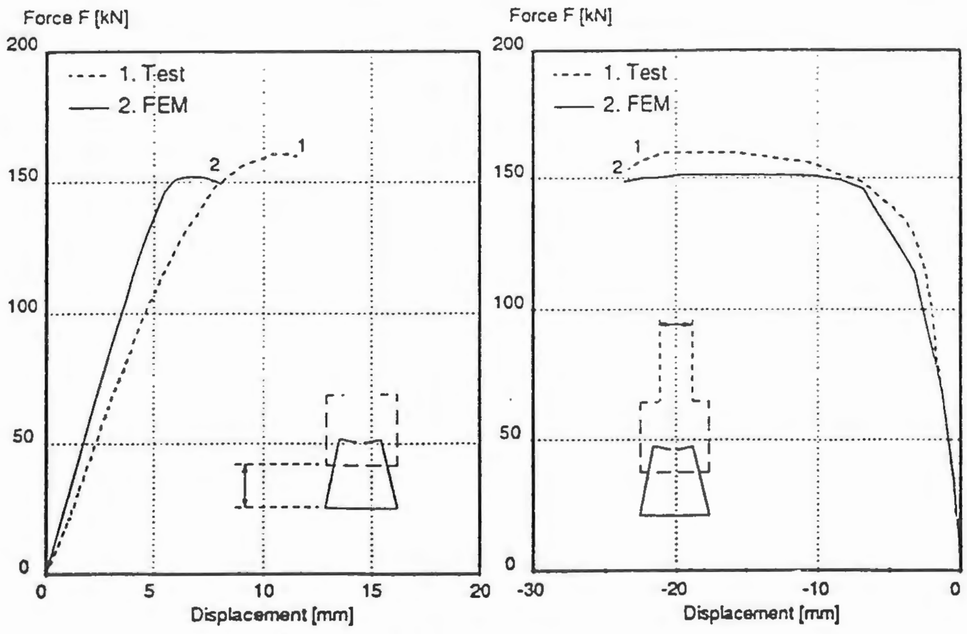


***Figure 10. C2/MR1***

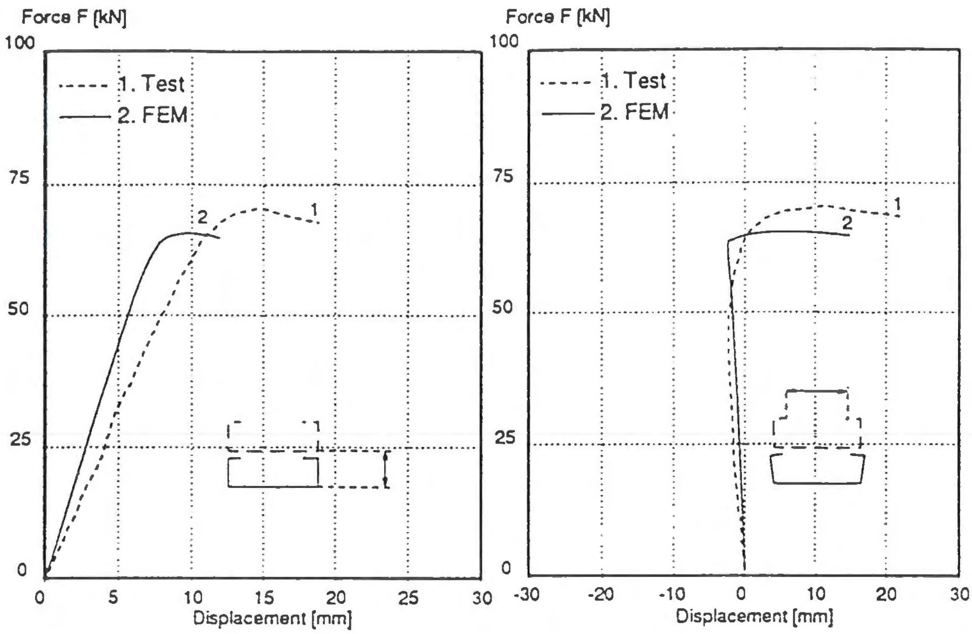


*Figure 11. C1/MR1*

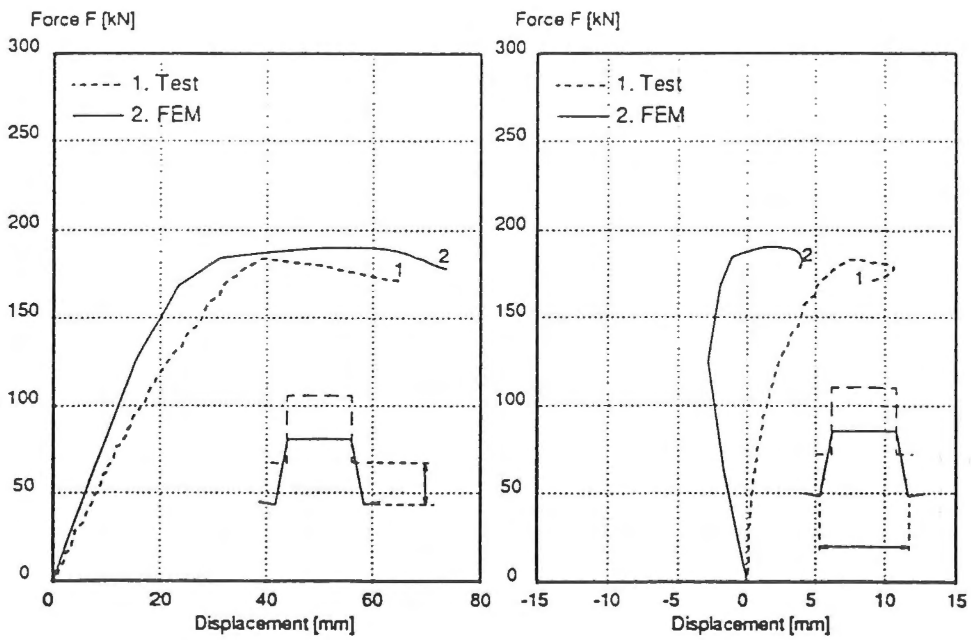


*Figure 12. H1/MR2*

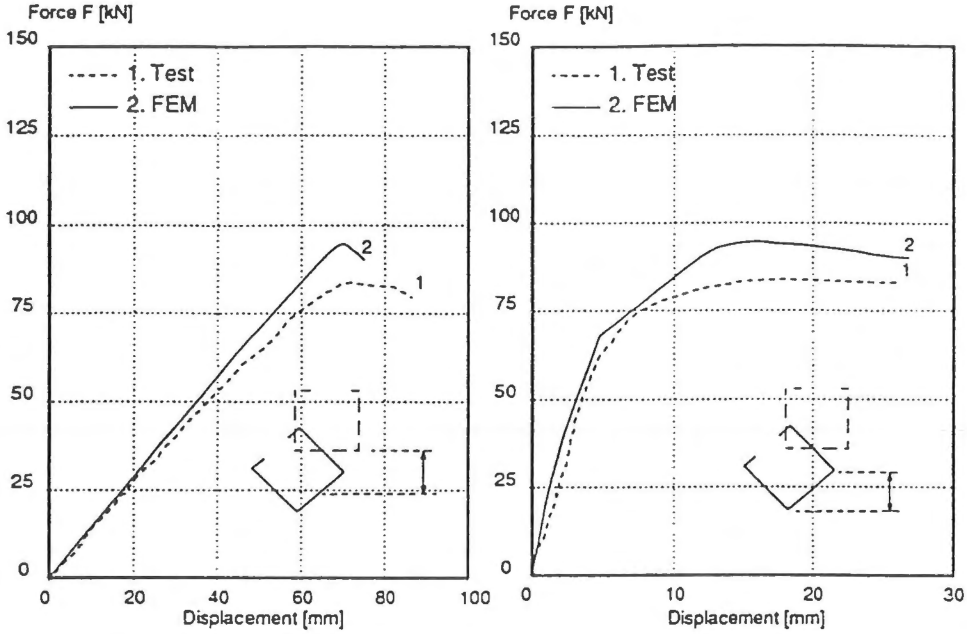


*Figure 13. C2/MR3*

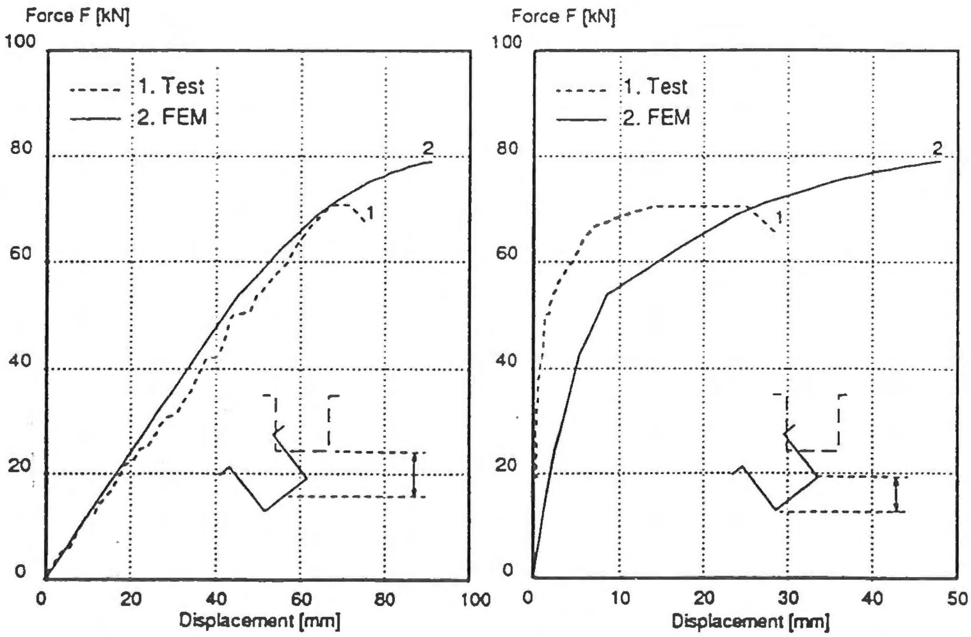


*Figure 14. H1/MR3*

*Table 4. Cross-sectional bending strength*

| Specimen | | F [kN] FEM | F [kN] Test | FEM / Test |
|---|---|---|---|---|
| MR1 | C1 | 65 | 71,5 | 0,91 |
| | C2 | 152 | 158,0 | 0,96 |
| | H1 | 158 | 141,5 | 1,12 |
| | H2 | 157 | 142,0 | 1,11 |
| MR2 | C1 | 75 | 76,0 | 0,99 |
| | C2 | 188 | 195,0 | 0,96 |
| | H1 | 190 | 185,0 | 1,03 |
| | H2 | 164 | 163,5 | 1,00 |

*Table 5. Lateral buckling strength*

| | Imperfection | F [kN] FEM | F [kN] Test | FEM / Test |
|---|---|---|---|---|
| C1 | - | 57 | 57,0 | 1,00 |
| | 100 % t (1.7°) | 58 | | |
| | 200 % t (3.5°) | 55 | | |
| C2 | - | 122 | | |
| | 50 % t (0.6°) | 111 | | |
| | 100 % t (1.3°) | 107 | | |
| | 200 % t (2.5°) | 95 | 84,5 | 1,12 |
| H1 | 100 % t (1.5°) | 83 | | |
| | 200 % t (2.9°) | 79 | 71,0 | 1,11 |
| H2 | 100 % t (1.7°) | 72 | | |
| | 200 % t (3.5°) | 66 | 59,0 | 1,12 |